UNCLASSIFIED

AD NUMBER
AD839681
LIMITATION CHANGES
TO: **Approved for public release; distribution is unlimited.**
FROM: **Distribution authorized to U.S. Gov't. agencies and their contractors; Critical Technology; SEP 1968. Other requests shall be referred to Atomic Energy Commission, Albuquerque Oprs Office, P. O. Box 5400, Albuquerque, NM 87115. This document contains export-controlled technical data.**
AUTHORITY
AEDC ltr, 23 Jan 1975

THIS PAGE IS UNCLASSIFIED

AEDC-TR-68-192

cy 1

SANDIA HIGH-PRESSURE ABLATION TEST IN THE AEDC 5-MEGAWATT ARC HEATER TEST UNIT SERIES III

J. R. Henson

ARO, Inc.

September 1968

PROPULSION WIND TUNNEL FACILITY
ARNOLD ENGINEERING DEVELOPMENT CENTER
AIR FORCE SYSTEMS COMMAND
ARNOLD AIR FORCE STATION, TENNESSEE

NOTICES

SANDIA HIGH-PRESSURE ABLATION TEST
IN THE
AEDC 5-MEGAWATT ARC HEATER TEST UNIT
SERIES III

J. R. Henson
ARO, Inc.

This document is subject to special export controls and each transmittal to foreign governments or foreign nationals may be made only with prior approval of AEC, Albuquerque Oprs Office, P.O. Box 5400, Albuquerque, New Mexico 87115.

This document has been approved for public release its distribution is unlimited. Per AF Letter dtd 23 Jan. 75 signed William O. Cole

FOREWORD

The test reported herein was sponsored by the Sandia Corporation under the Atomic Energy Commission (AEC), Contract No. ASB 6007-009 (AL 67-255). The controlling office is AEC, Albuquerque Oprs Office, P. O. Box 5400, Albuquerque, New Mexico. The Program Area is 920D.

The results of the test presented were obtained by ARO, Inc. (a subsidiary of Sverdrup & Parcel and Associates, Inc.), contract operator of the Arnold Engineering Development Center (AEDC), Air Force Systems Command (AFSC), Arnold Air Force Station, Tennessee, under Contract F40600-69-C-0001. The test was conducted in the 5-Megawatt Arc Heater Test Unit of the Propulsion Wind Tunnel Facility from June 3 to June 7, 1968, under ARO Project No. PL1890, and the manuscript was submitted for publication on August 5, 1968.

~~Information in this report is embargoed under the Department of State International Traffic in Arms Regulations. This report may be released to foreign governments by departments or agencies of the U. S. Government subject to approval of the U. S. Atomic Energy Commission, Albuquerque Oprs Office, or higher authority. Private individuals or firms require a Department of State export license.~~

This technical report has been reviewed and is approved.

Richard W. Bradley
Lt Colonel, USAF
AF Representative, PWT
Directorate of Test

Roy R. Croy, Jr.
Colonel, USAF
Director of Test

ABSTRACT

Six ablation test runs, involving 30 models, were made in an arc-heated free-jet facility using air as the test fluid. The test was conducted to screen and examine the ablation performance of various materials with different microscopic structures. The investigation was accomplished at Mach numbers of 1.6, 2.0, and 2.3 with measured reservoir pressures ranging from 51.1 to 99.0 atm and enthalpies from 3435 to 2315 Btu/lb. The models were hemisphere-cylinder specimens of composite materials. The data measured during the present investigation are presented in a documentary manner with a minimum of analysis because the composition of the specimen material is proprietary. The models are referred to by number designation only.

CONTENTS

APPENDIXES

NOMENCLATURE

h_t	Total enthalpy, Btu/lb
I	Arc heater current, amp
L_h	Power loss to arc heater cooling water, kw
L_n	Power loss to nozzle cooling water, kw
$\dot{m}$	Air mass flow rate, lb/sec
P	Power to arc heater, kw
p_s	Model stagnation pressure, atm
p_t	Arc heater reservoir pressure, atm
V	Arc heater voltage, v
ΔL	Change in model length by ablation, in.
Δm	Change in model mass by ablation, gm
ΔT	Cooling water temperature rise, °F
Δt_m	Model dwell time, sec
η	Arc heater efficiency

SECTION I
INTRODUCTION

The primary objectives of the Sandia ablation program were to examine the ablation performance of materials with different microscopic structures and to determine the change that occurs during ablation under high pressure and temperature. The accomplishment of these objectives was supported by ablation testing in the 5-Megawatt Arc Heater Test Unit of the Propulsion Wind Tunnel Facility (PWT) at the Arnold Engineering Development Center.

The physical composition of the models investigated and reported on herein is proprietary to the Sandia Corporation. A further description of the model composition is available from the Sandia Corporation.

This report presents the documented test results, a description of the test facility, model configuration, instrumentation, and operational procedure for the test program.

SECTION II
DESCRIPTION OF TEST APPARATUS

2.1 5-MEGAWATT ARC HEATER TEST UNIT

The 5-Megawatt Arc Heater Test Unit[1] is a continuous-flow, arc-heated facility using air and is equipped for ablation tests over a wide range of reentry conditions. An electrical line diagram with power supply, ballast, and arc heater is shown in Fig. 1, Appendix I. The test unit configuration consists of the arc heater, nozzle, model injection system, and exhaust ducting (Fig. 2).

A sectional view of the arc heater is shown in Fig. 3. The heater consists of two water-cooled coaxial electrodes separated by a cylindrical swirl chamber. The rear electrode (silver-copper alloy) is the anode and the front electrode (tough pitch copper) is the cathode. Demineralized water is used to cool the electrodes during heater operation.

---

[1] Test Facilities Handbook (Seventh Edition). "Propulsion Wind Tunnel Facility, Vol. 5." Arnold Engineering Development Center, July 1968.

Air flows into the swirl chamber through six tangentially oriented orifices and passes through the cathode, generating a vortex which rotates the termination of the arc column and provides a centrifuged layer of cooler air at the cathode surface. The coil surrounding the anode generates a magnetic field which interacts with the column to augment the rotation of the arc termination in the anode and minimize loss of anode material.

Supersonic water-cooled nozzles are used to provide a free jet at Mach numbers of 1.6, 2.0, and 2.3 at the nozzle exit plane. The convergent sections of the nozzles are conical and are joined to circular arc sections which extend to the throat. The nozzle expansion sections are contoured to produce uniform, parallel flow. The nozzle discharges to atmosphere, and the values of reservoir pressure are such that the nozzle operates underexpanded. A sectional view of the nozzle assembly, showing a typical nozzle liner (Mach 2.0), outer shell, and cooling water passages, is presented in Fig. 4.

A multiple-head, laterally moving injection system injects from one to five models into the jet stream for a preset dwell time from 1.0 to 15 sec. The support system is hydraulically actuated and remotely controlled. Arc chamber conditions remain constant for all models, and transit time is approximately 0.50 sec from position to position. The maximum deceleration of the model injection system is approximately 120 ft/sec^2. The injection of the models transverse to the axis of the jet minimizes the transit time from the boundary to the center of the jet. A photograph of the multiple-head injection system is shown in Fig. 5.

The exhaust system consists of an inlet section, a short section of water-jacketed ducting (36-in.-ID), a section of uncooled ducting of 36-in. ID, and a vertical duct of 20-in. ID with a single-stage, axial-flow fan discharging to atmosphere.

2.2 TEST UNIT INSTRUMENTATION

Test unit instrumentation consists of visual indicators and recording equipment. Visual observation of pressures is accomplished by use of Autosyn® transmitters and indicators. Test unit temperatures are monitored by various types of thermocouples. Water flow rates are measured with turbine-type flowmeters and pulse rate converters. Arc voltage and current are measured by use of a voltage divider and a current shunt. A 36-channel recording oscillograph is used to record all data necessary

to calculate arc heater performance. A closed-circuit television system is used to view the models during each test run.

2.3 MODEL INSTRUMENTATION

Brightness temperatures of the model ablating surface, while being exposed to the heater flow and during model cooldown, are measured by miniature pyrometers[2], which were developed and fabricated by the Johns Hopkins Applied Physics Laboratory. The outputs from the sensors are recorded by oscillograph recorders.

Three motion picture cameras are used for model ablation documentation. These are 16-mm cameras using color film and operating at speeds up to 600 frames/sec. Camera locations, lens settings, types of filters, film and operating speeds are presented in Table I, Appendix II.

Data from the recording oscillographs and cameras may be correlated from timing marks generated by a transistorized timing signal device. The models themselves were not physically instrumented with thermocouples or pressure taps.

2.4 DESCRIPTION OF MODELS

All models were furnished by the Sandia Corporation. The ablation specimen configuration was a hemisphere-cylinder. The hemisphere nose radius was 0.20 in.; the cylinder diameter was 0.40 in. A typical pretest photograph of an ablation specimen is shown in Fig. 6.

The specimen holder was fabricated from phenolic Refrasil® molded in a truncated cone-cylinder configuration. The cylinder diameter was 2.5 in. Components of a typical ablation model are shown in Fig. 7.

SECTION III
TEST PROCEDURE

3.1 MODEL PREPARATION

All ablation specimens were weighed, measured, photographed, and assembled with the holders by Sandia personnel before being installed for

---

[2]Hill, M. L., Akridge, J. M. and Keeler, C. A. "Miniature Recording Optical Pyrometer." Johns Hopkins University Applied Physics Laboratory, Report TG-825 (AD636101), May 1966.

testing. The weights and measurements of the specimens are presented in Table II. Models were installed on the injection system with the nose tip positioned 0.050 in. axially from the nozzle exit plane. The centerline of the models was aligned to the centerline of the nozzle. The position of the models with respect to the nozzle is shown in Fig. 8.

After the test was completed, the models were photographed and returned to the Sandia Corporation to be disassembled, weighed, and measured. Posttest weights and lengths of the specimens are also presented in Table II. These measurements were made by the Sandia Corporation.

3.2 TYPICAL RUN

Prerun electrical calibrations were made of the arc heater unit and model instrumentation. The arc heater data-recording equipment was started, then cooling water flow, heater airflow, and current flow to the arc heater magnetic coil were initiated. The arc was energized by applying open-circuit voltage and moving the carbon-tipped starting rod to the anode seal shield (Fig. 3). The power level (using the tap-changing-under-load transformer) and airflow were adjusted to the required levels, and approximately 20 sec were allowed for the cooling water discharge temperatures to stabilize. At this time, the model data-recording equipment and motion picture cameras were started. The models were then injected for a preset dwell time. After all the models had been injected, the heater power was shut off and a postrun electrical calibration of the instrumentation was performed.

SECTION IV
RESULTS

4.1 RUN SUMMARY

A summary of the six runs is presented in Table III, which includes pertinent model description, instrumentation, and dwell time information as recorded on the 36-channel oscillograph. The runs were accomplished at Mach numbers of 1.6, 2.0, and 2.3 with reservoir pressures ranging from 51.1 to 99.9 atm and enthalpies from 3435 to 2315 Btu/lb.

4.2 HEATER TEST CONDITIONS

4.2.1 Measurement and Calculation of Test Conditions

The input voltage and current are measured using a voltage divider and a current shunt. It is estimated that the uncertainty in determining

the average arc power input from these measurements is ±3 percent. Additional inaccuracies are caused by arc current and voltage fluctuations.

Air mass flow rates ($\dot{m}$) are measured by use of a choked venturi meter (0.110-in.-diam throat) built to American Society of Mechanical Engineers standards. Above 40 atm reservoir pressure, however, mass flow rates are calculated using the measured pressure and temperature at the inlet to the six tangentially oriented orifices through which air enters the arc heater (Fig. 3). These orifices are operated in the choked condition and were calibrated with a choked venturi built to ASME standards. It is estimated that the uncertainty in measuring air mass flow is ±4 percent.

Total (reservoir) pressure (p_t) in the arc heater is measured by means of a wall pressure orifice in the heater swirl chamber located in the front shell seal. Some uncertainty is inherent in the pressure measurement because of the swirl velocity present. The estimated uncertainty in measuring p_t is ±2 percent.

Total enthalpy (h_t) is calculated as follows:

$$h_t = 0.948 \frac{P - L_h - L_n}{\dot{m}} + 100 \text{ Btu/lb}$$

The first term is the net enthalpy increment given the air by the arc heater and includes energy losses to the arc heater and nozzle cooling water. The number 0.948 is to convert from electrical to thermal units. The second term in the equation is the ambient enthalpy of the incoming air. Power to the arc (P) is obtained from arc voltage and current measurements. The energy loss to the arc heater cooling water (L_h) is the sum of the anode and cathode losses, and L_n is the nozzle loss. Cooling water ΔT's are measured by thermistors with opposed emf and whose bridge circuits incorporate passive shaping elements designed to made the thermistor outputs linear over the ΔT range from 0 to 40°F. Values of ΔT derived from differential thermocouples (copper/constantan) are used as alternate measurements or are used when the cooling water ΔT exceeds 40°F. Combining all the uncertainties in measurements, it is estimated that the calculated total enthalpy values given in Table IV may be in error by ±10 percent.

4.2.2 Facility Repeatability

Target heater conditions for the six runs were enthalpies of 3500 Btu/lb at a reservoir pressure of 50 atm and 2400 Btu/lb at 90 and 100 atm. The heater conditions attained during the test are presented in Table IV. In view of the fact that enthalpy is affected by such things as the variation

in voltage on the primary side of the 30,000-kva transformer (Fig. 1), surface conditions of the heater electrodes, purity of the air, and accuracy of the mass flow measurement, the resulting repeatability is considered to be acceptable.

4.3 SPECIMEN RECESSION AND MASS LOSS

The average recession rate and mass loss rate for the ablation specimens investigated are presented in Table V. The recession rate is the change in specimen length per unit exposure time. The mass loss rate is the change in specimen mass per unit exposure time. These parameters and the posttest photographs, presented in Fig. 9, provide a good comparative index from which a relative ranking of materials can be made within a run or runs at similar test conditions. The specimens which exhibited superior performance were IP-22E-68-1, IP-17-66-1, 5Q-22, and IP-17-26-1. It should be noted that all of the IP-designated models exhibited good ablation characteristics.

The ranking of model materials by average recession rates and mass loss rates does not rule out other specimens for further consideration. A complete evaluation of the ablation materials should be based on instantaneous ablation rates and should include such material properties as thermal conductivity, density, strength, and composition. An extensive study of each material is being conducted by the Sandia Corporation.

4.4 PYROMETER DATA

The brightness temperature of the ablating surfaces of the specimen during exposure to heater flow and of the surface cooldown in next lock position after being exposed to heater flow were recorded by pyrometers. The maximum recorded temperatures from each specimen during exposure are presented in Table VI. A typical surface brightness temperature history of a specimen during heater exposure is presented in Fig. 10. After the specimen ablated past the pyrometer alignment point, the pyrometer output decreased sharply; therefore, the maximum temperature recorded is the most valid value. The surface brightness temperatures recorded during cooldown for each specimen are presented versus time in Fig. 11. The pyrometer is aligned on the ablated stagnation point of the specimen in the next lock position after being exposed to the heater flow. The filter was removed from this pyrometer for better accuracy at lower temperatures.

APPENDIXES

I. ILLUSTRATIONS

II. TABLES

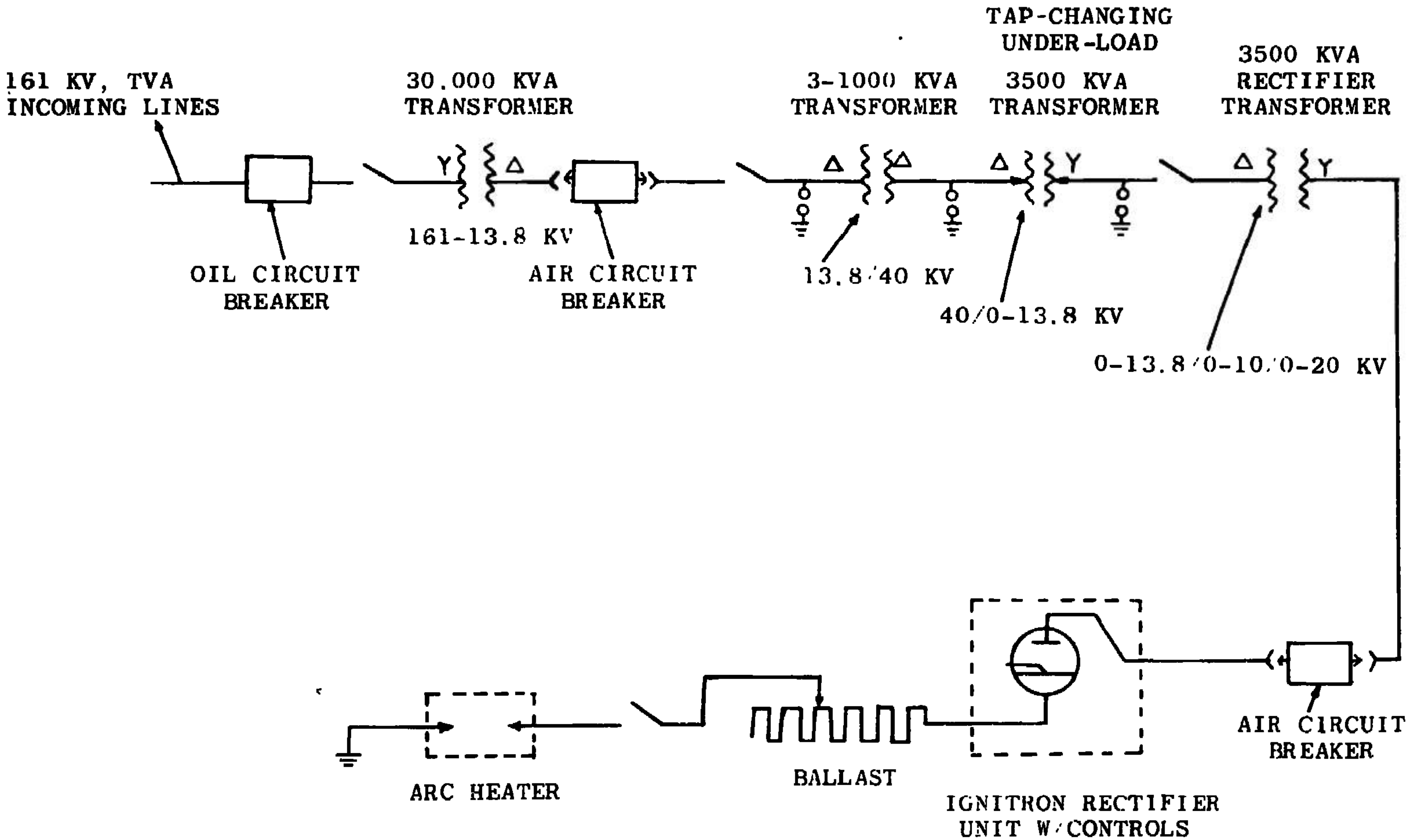

Fig. 1 Main Power-Supply Line Diagram

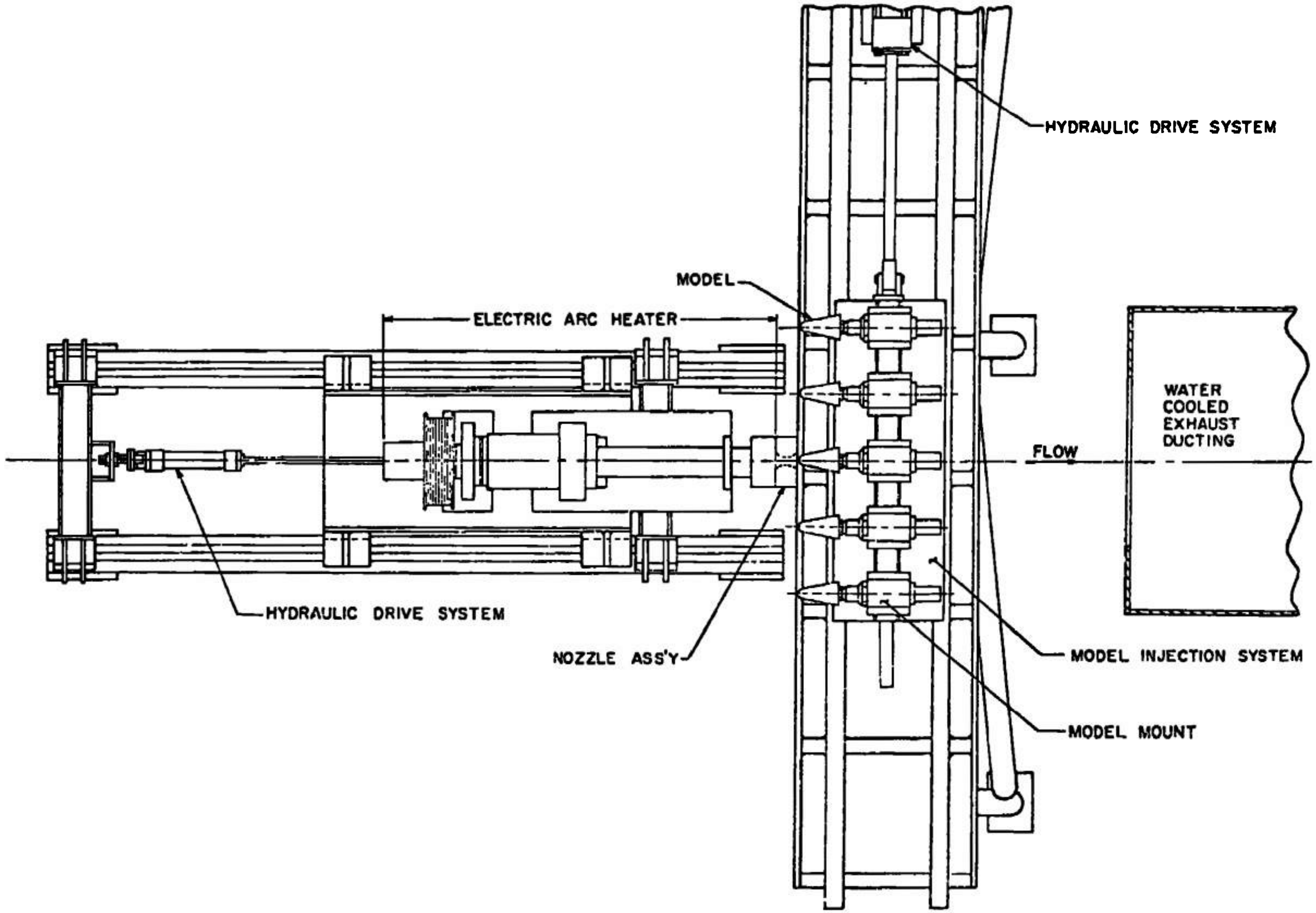

Fig. 2 5-Megawatt Arc Heater Test Unit

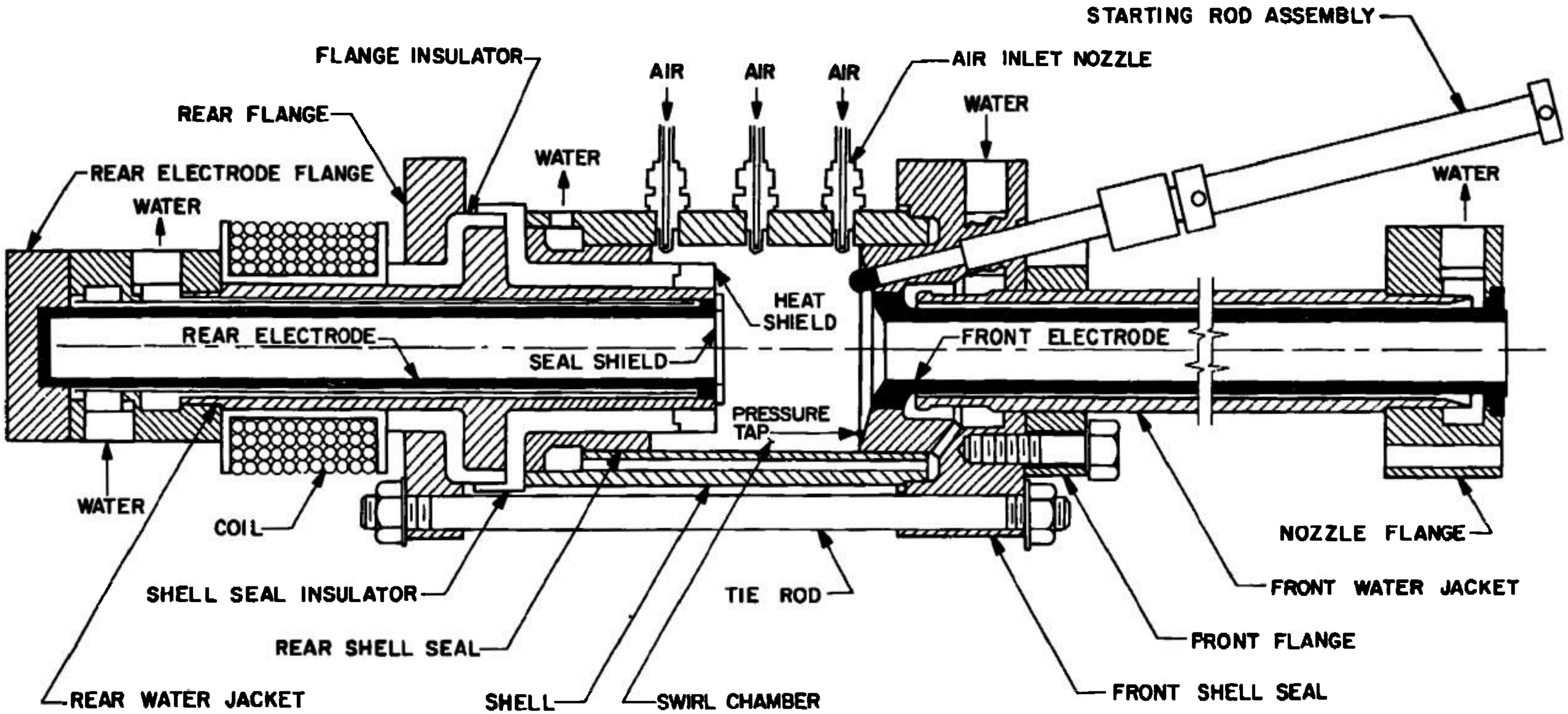

Fig. 3 Schematic of Modified Linde N-4000 Arc Heater

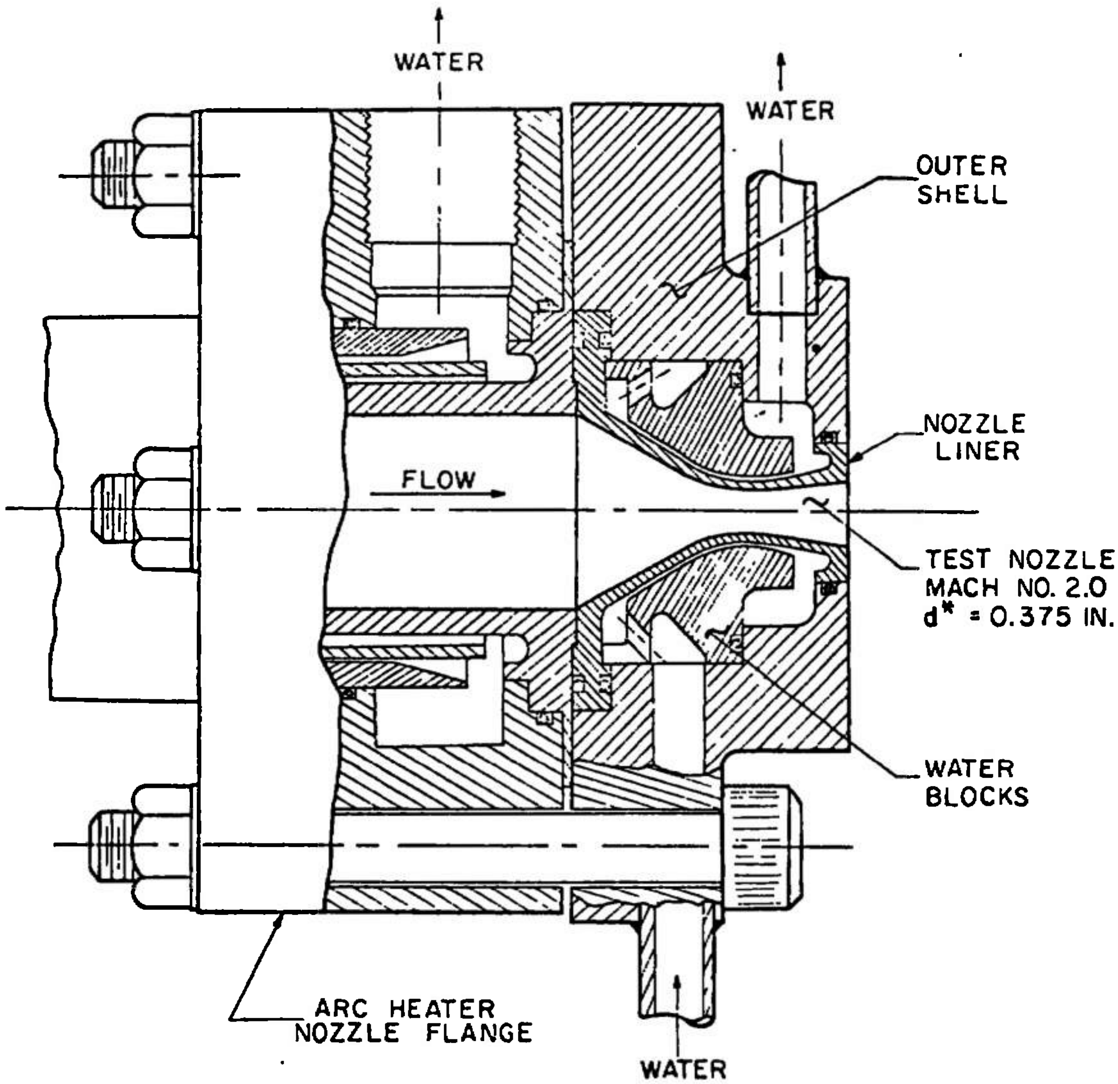

Fig. 4 Typical Nozzle Configuration

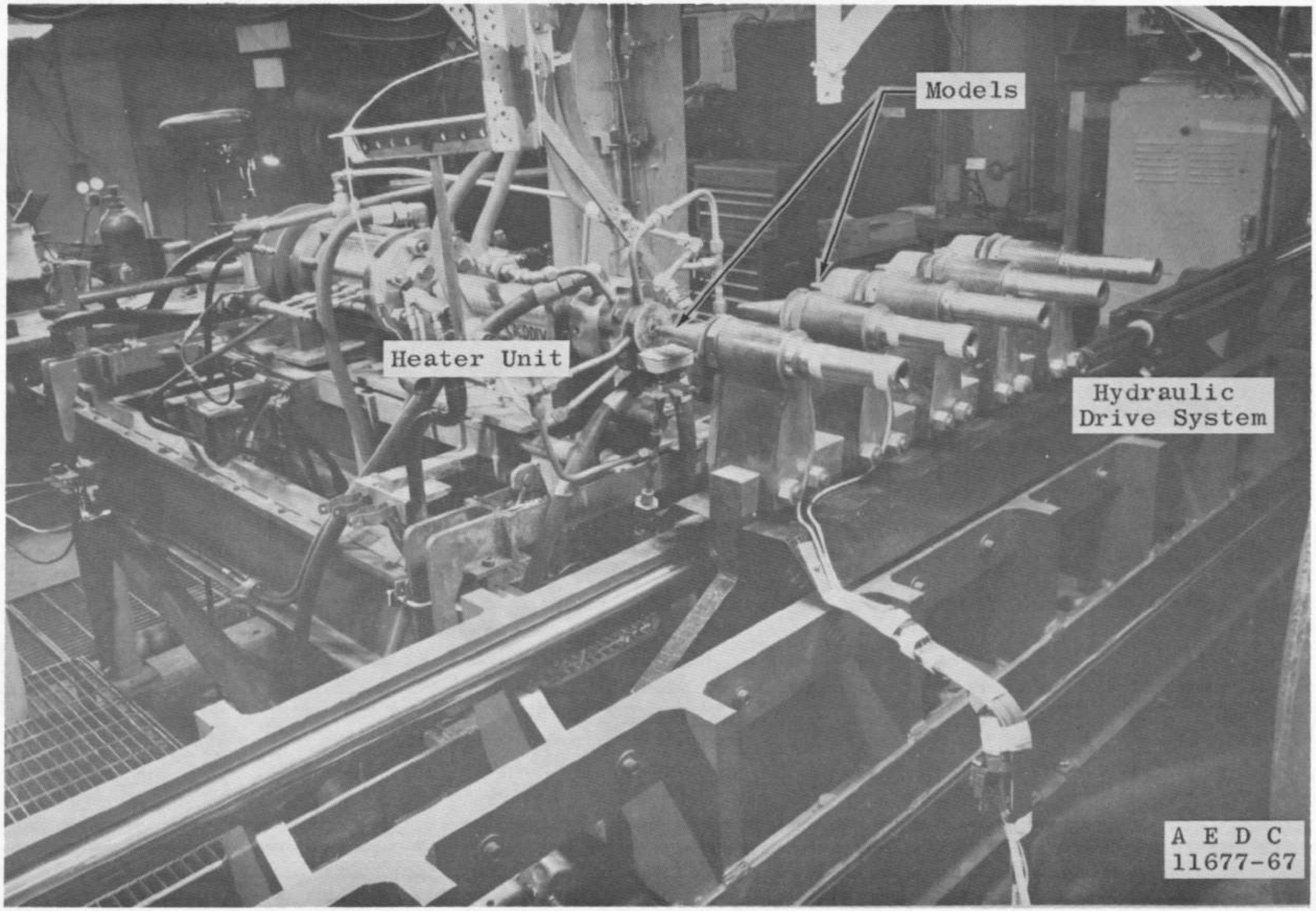

Fig. 5 Multiple-Head Injection System

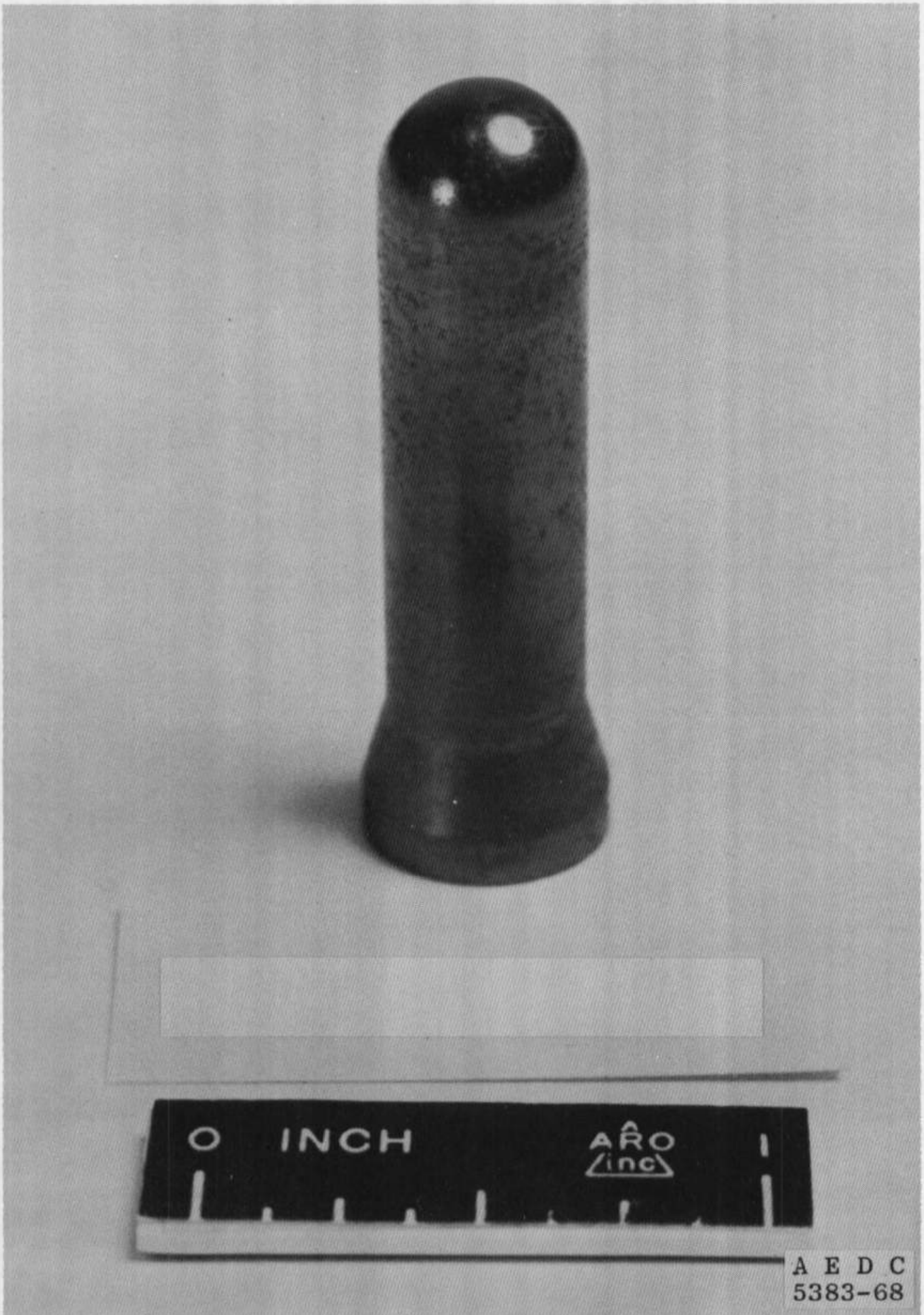

Fig. 6 Ablation Specimen Photograph

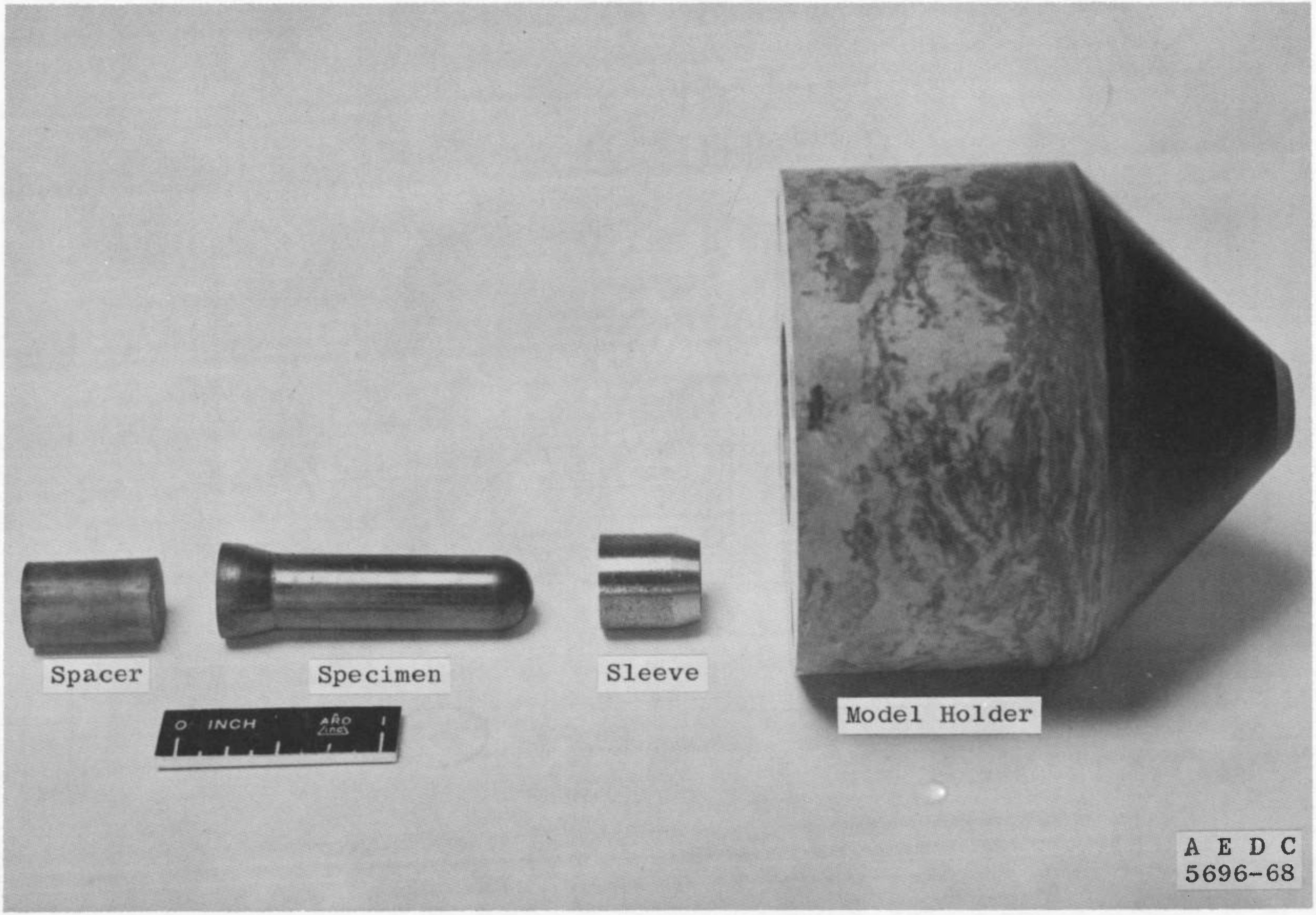

Fig. 7 Ablation Model Components

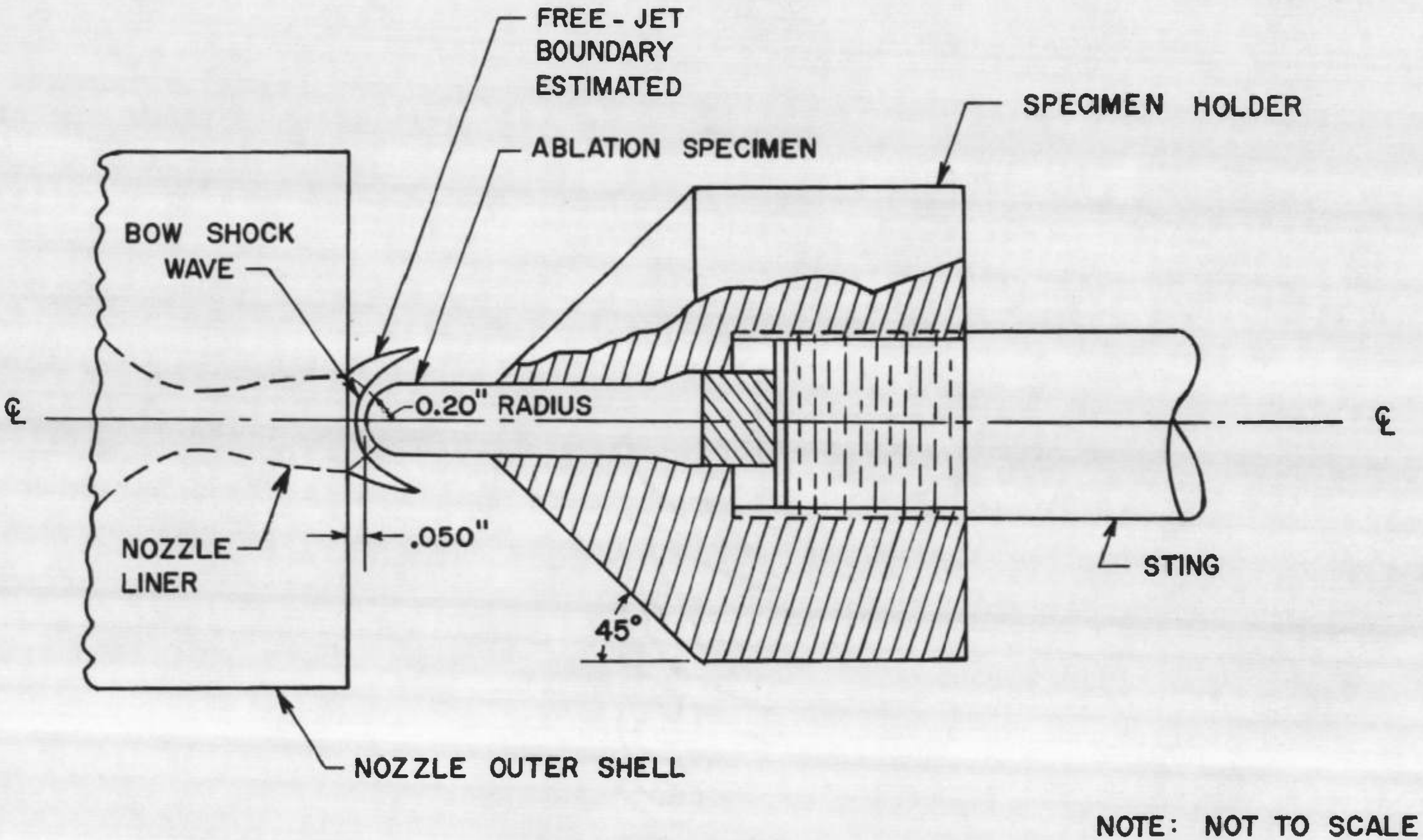

Fig. 8 Side View of Model in Test Position

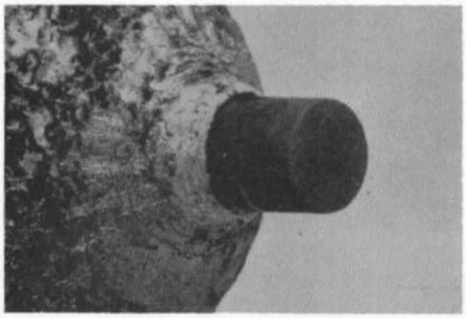

1. Model ATJ-S1

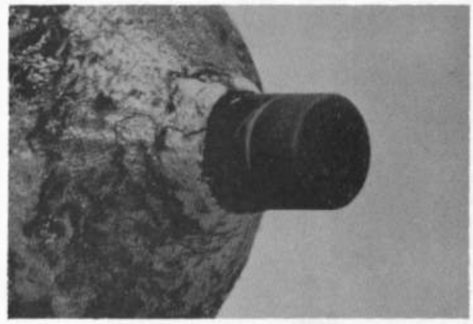

2. Model ATJ-S2

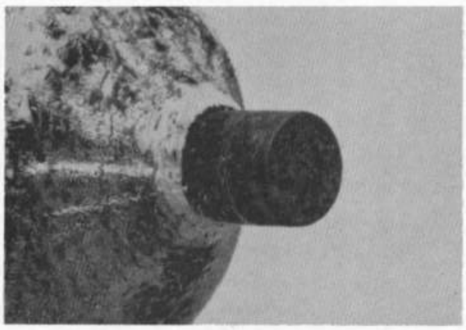

3. Model IP-22E-67-2

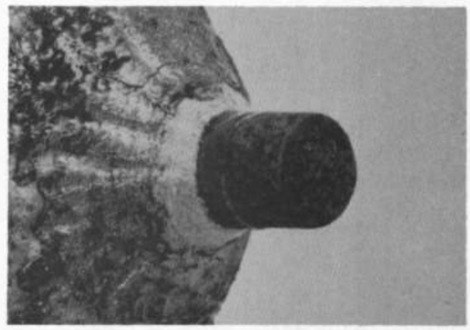

4. Model IP-22E-68-2

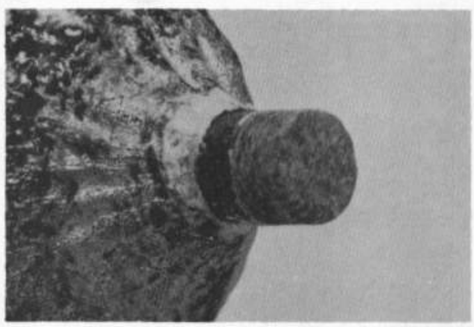

5. Model IP-22C-71-2

a. Run S-8

Fig. 9 Posttest Photographs of Ablation Models

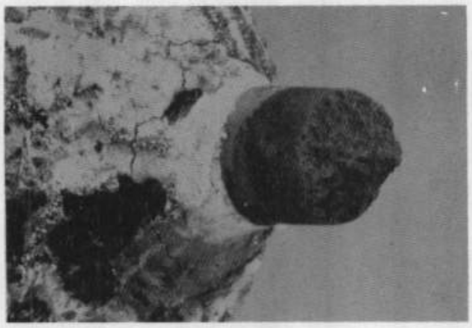

1. Model ATJ-S3

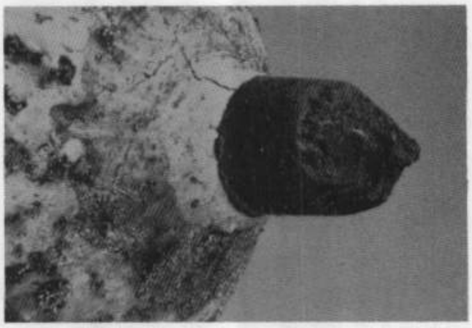

2. Model ATJ-S4

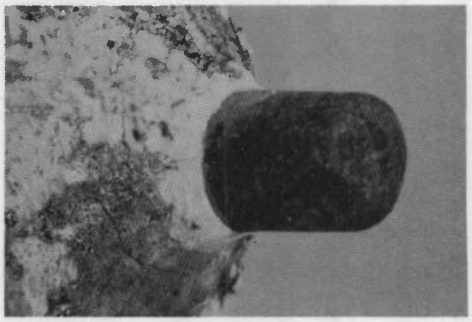

3. Model IP-17-26-1

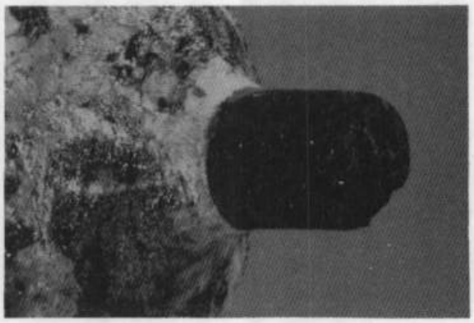

4. Model IP-17-27-1

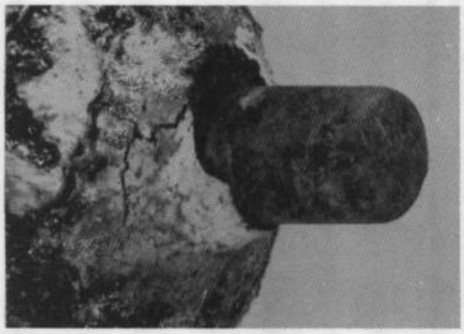

5. Model IP-17-66-1

b. Run S-9

Fig. 9 Continued

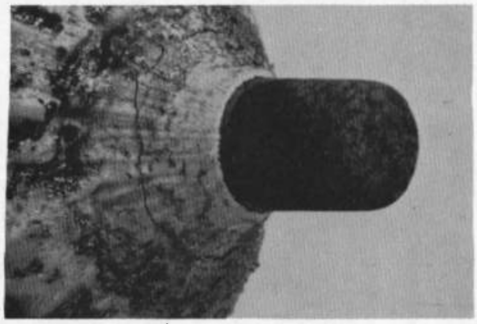

1. Model IP-22E-67-1

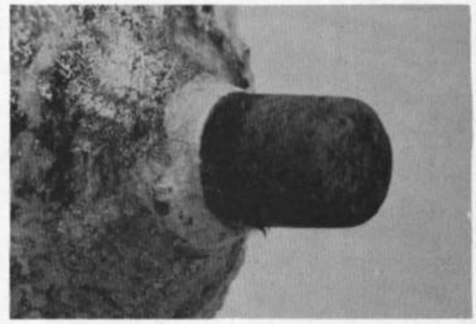

2. Model IP-22E-68-1

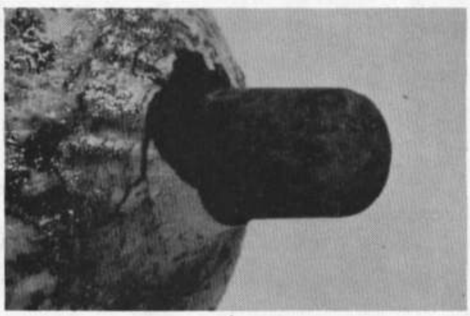

3. Model IP-22F-69-1

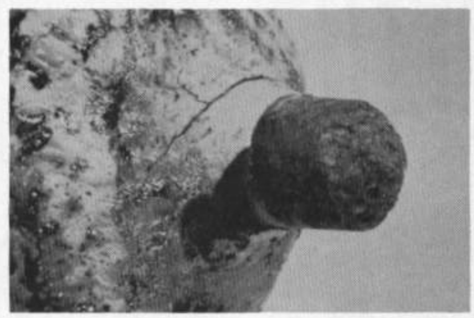

4. Model IP-22C-70-1

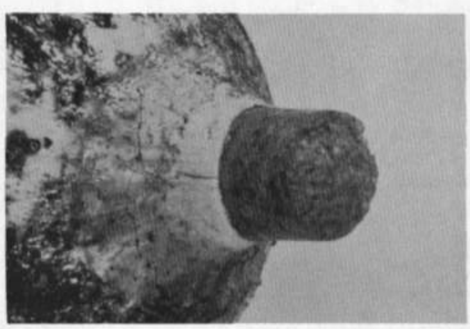

5. Model IP-22C-71-1

c. Run-S10A

Fig. 9 Continued

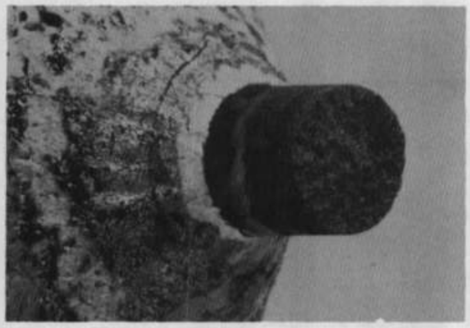

1. Model ATJ-S5

2. Model 5Q-12

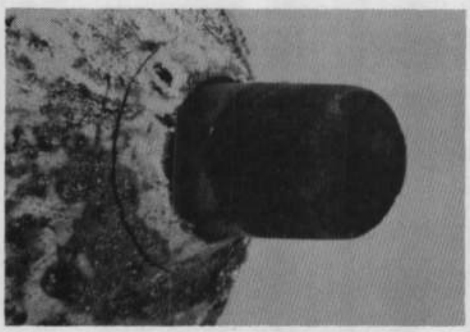

3. Model 5Q-22

4. Model IP-22E-67-3

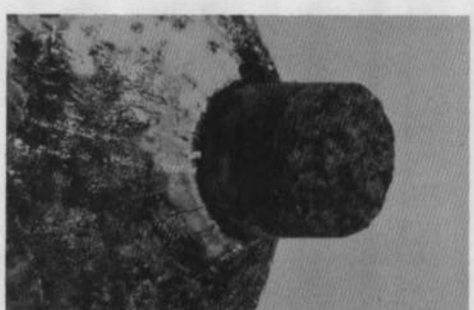

5. Model IP-22E-68-2F

d. Run S-11

Fig. 9 Continued

1. Model ATJ-S6

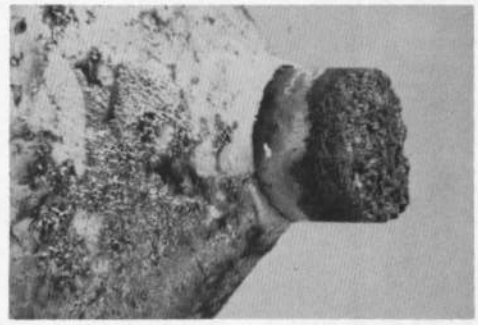

2. Model CVD-1A

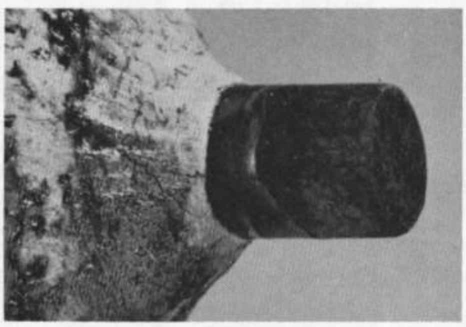

3. Model IP-22E-67-4

4. Model IP-22F-69-2

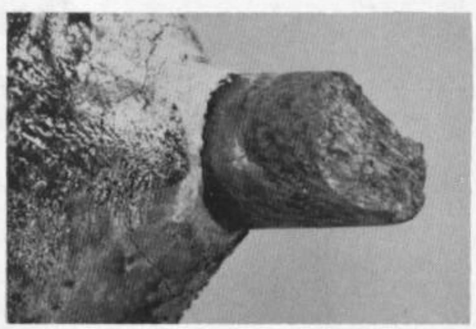

5. Model IP-22F-69-3

e. Run S-12A

Fig. 9 Continued

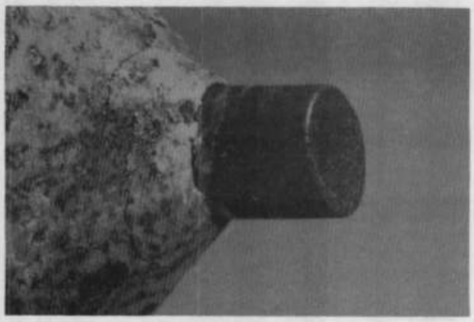

1. Model ATJ-S7

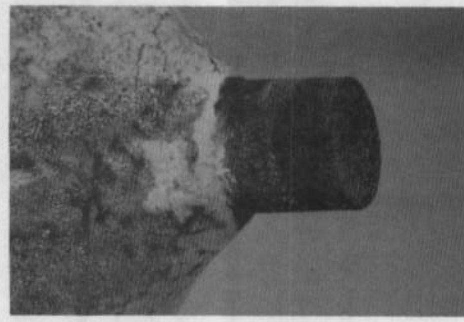

2. Model ATJ-S8

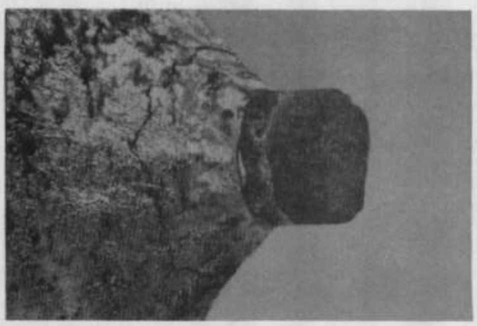

3. Model CVD-1B

4. Model IP-22F-69-4

5. Model IP-22C-70-3

f. Run S-13

Fig. 9 Concluded

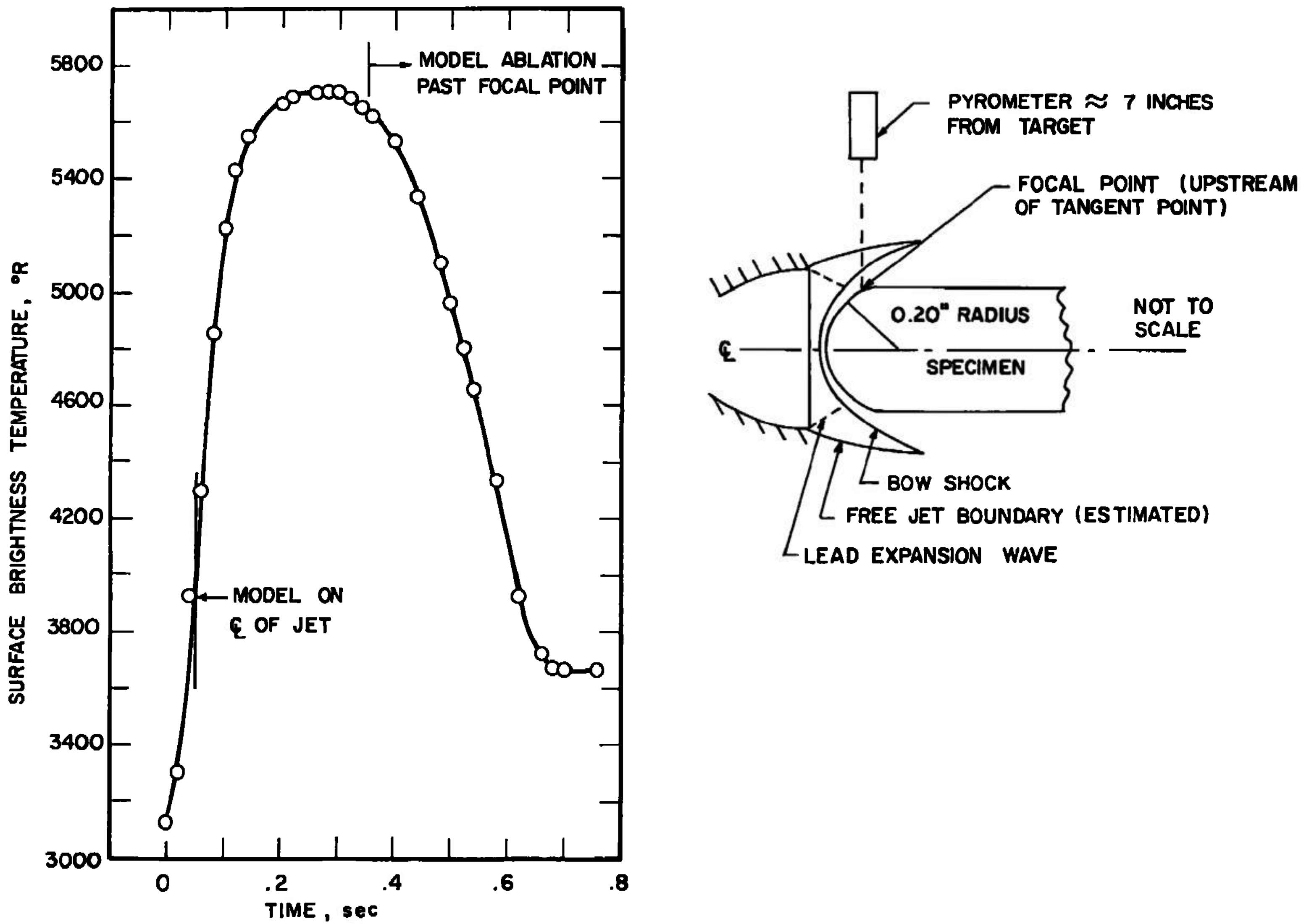

Fig. 10 Typical Surface Brightness Temperature History

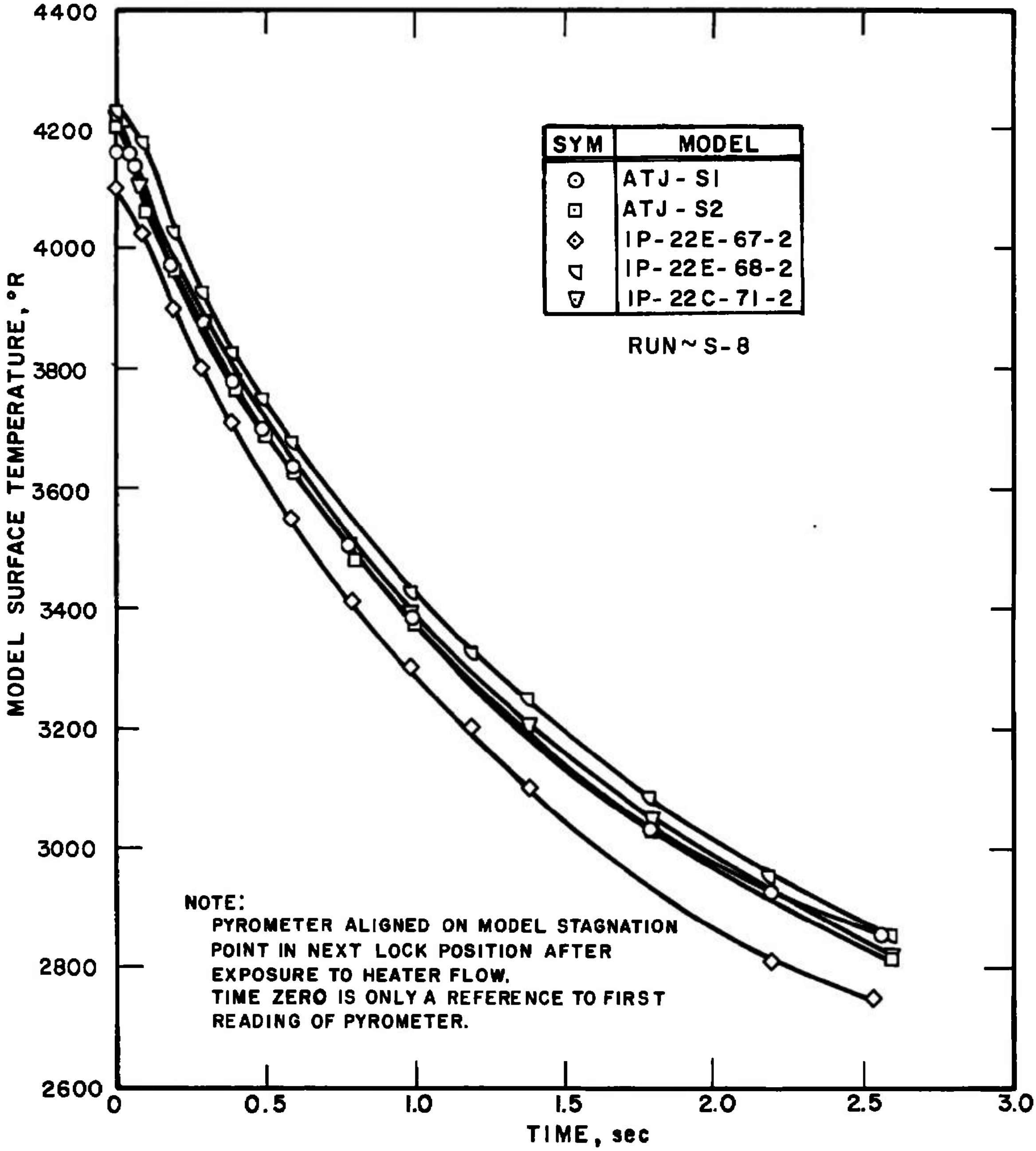

a. Run S-8

Fig. 11 Model Cooldown Pyrometer Data

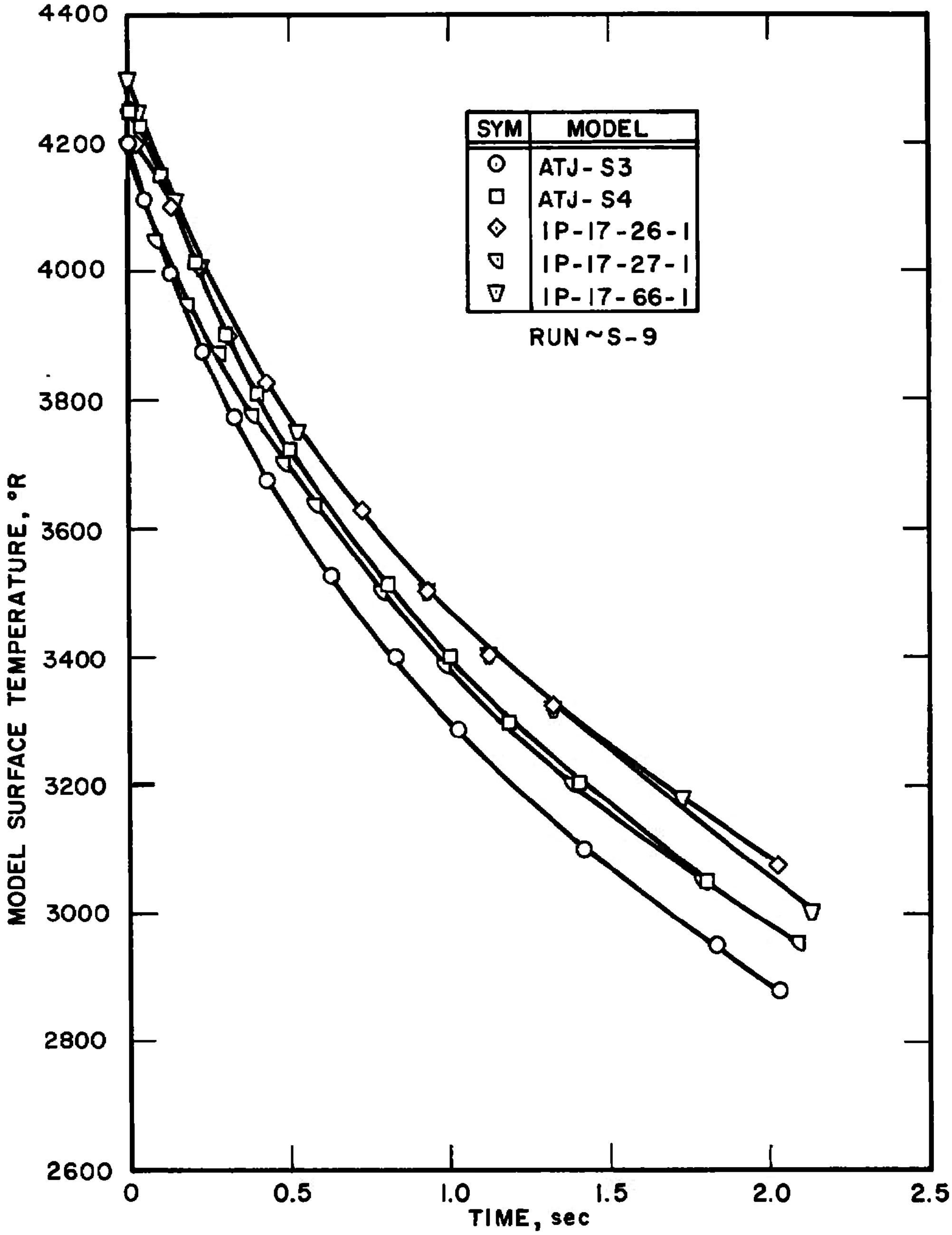

b. Run S-9

Fig. 11 Continued

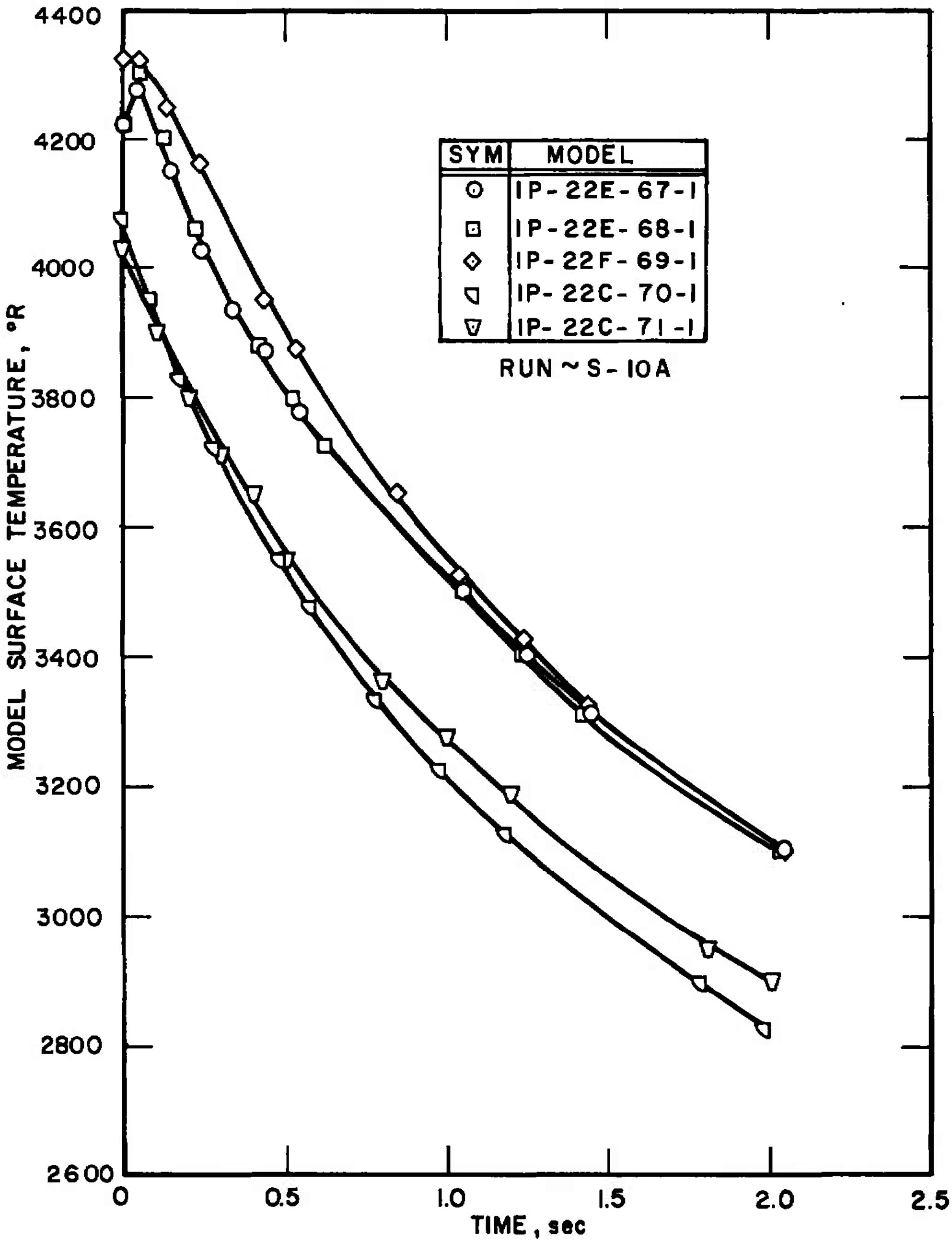

c. Run S-10A

Fig. 11 Continued

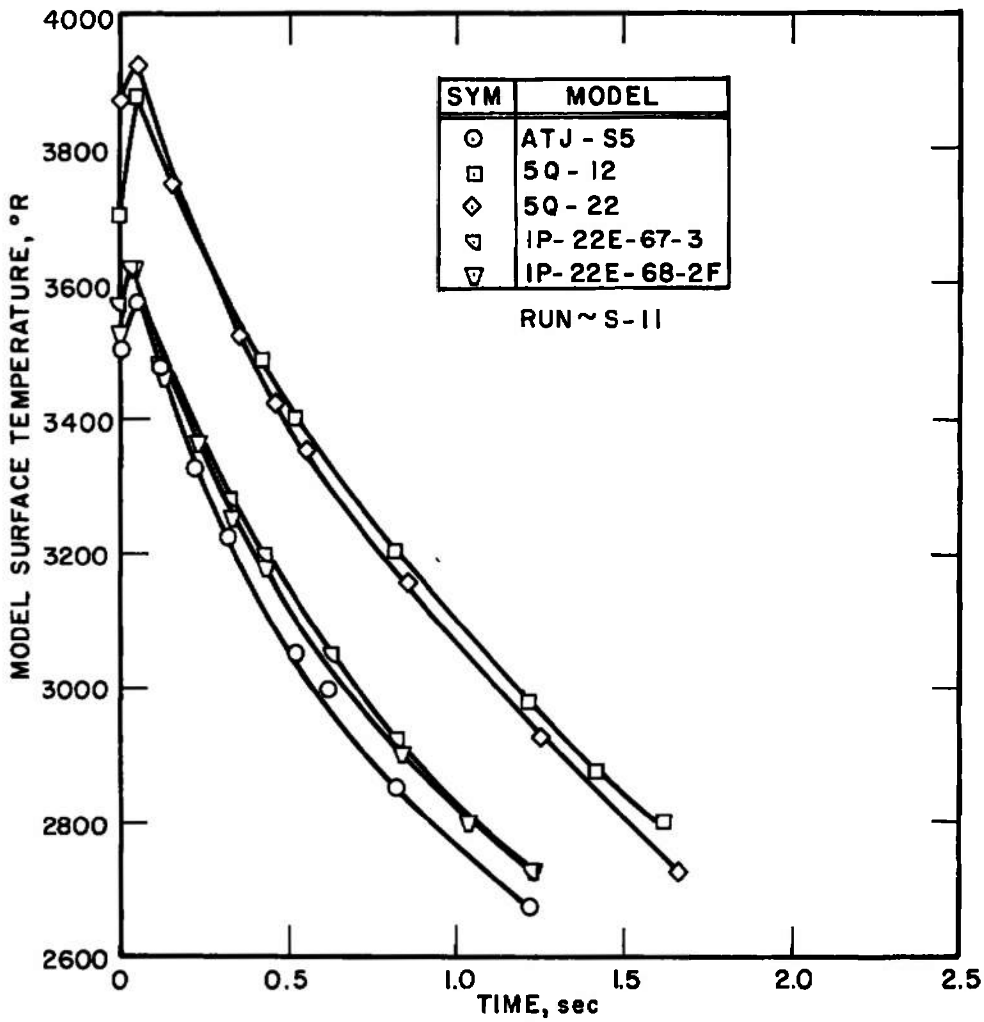

d. Run S-11

Fig. 11 Continued

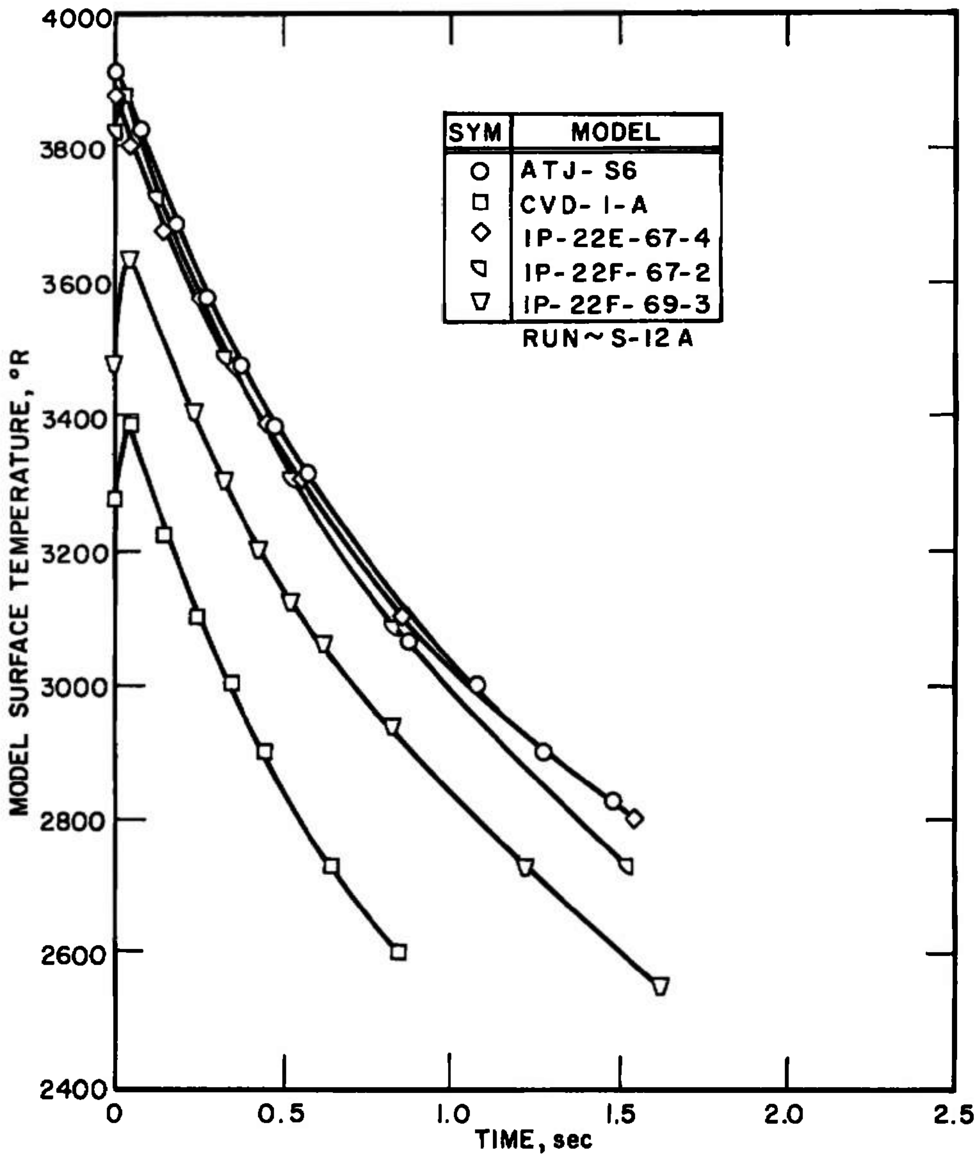

e. Run S-12A

Fig. 11 Continued

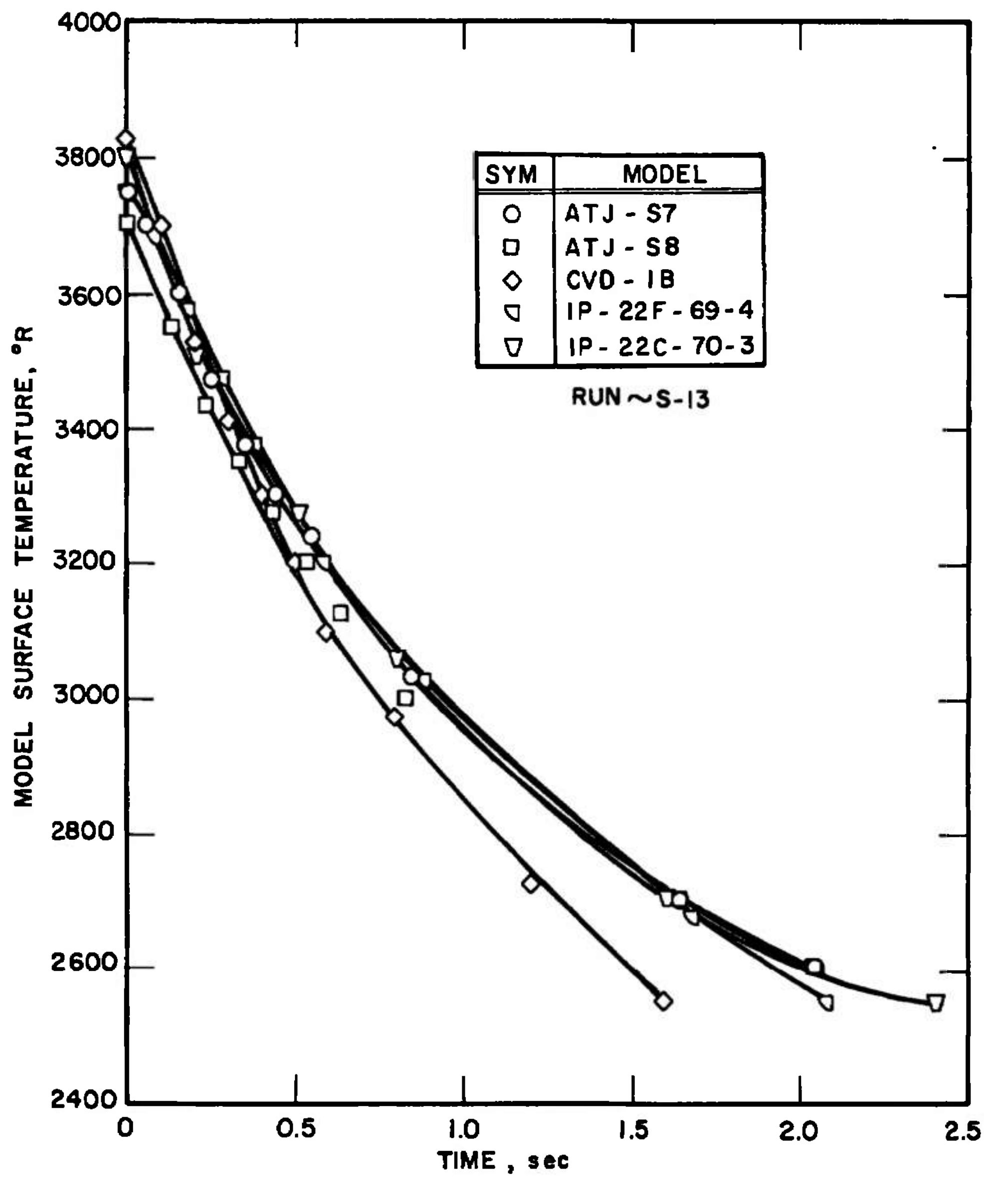

f. Run S-13

Fig. 11 Concluded

TABLE I
MOTION PICTURE LOG

Run No.	Camera No.	Camera Type	Film Type	Camera Speed, fps	Focal Length, in.	F/Stop	Filter	Shutter	Remarks
S-8	1	Hycam	7256	600	8	22	1.40/0 N.D.	10/1	
	2	D. B. Milliken	7256	400	6	22	0.30 N.D.	18 deg	
	3	D. B. Milliken	7256	400	8	22	0.90 N.D.	7.5 deg	
S-9	1	Hycam	7256	600	8	22	1.40/0 N.D.	10/1	
	2	D. B. Milliken	7256	400	6	22	0.30 N.D.	18 deg	
	3	D. B. Milliken	7256	400	8	22	0.90 N.D.	7.5 deg	
S-10A	1	Hycam	7256	600	8	22	1.40/0 N.D.	10/1	
	2	D. B. Milliken	7256	400	6	22	0.30 N.D.	18 deg	
	3	D. B. Milliken	7256	400	8	22	0.90 N.D.	7.5 deg	
S-11	1	Hycam	7256	600	8	22	1.40/0 N.D.	10/1	
	2	D. B. Milliken	7256	400	6	22	0.30 N.D.	18 deg	
	3	D. B. Milliken	7256	400	8	22	0.90 N.D.	7.5 deg	
S-12A	1	Hycam	7256	600	8	22	1.40/0 N.D.	10/1	Camera did not run.
	2	D. B. Milliken	7256	400	6	22	0.30 N.D.	18 deg	
	3	D. B. Milliken	7256	400	8	22	0.90 N.D.	7.5 deg	
S-13	1	Hycam	7256	600	8	22	1.40/0 N.D.	10/1	
	2	D. B. Milliken	7256	400	6	22	0.30 N.D.	18 deg	
	3	D. B. Milliken	7256	400	8	22	0.90 N.D.	7.5 deg	

TABLE II
SPECIMEN PRETEST AND POSTTEST WEIGHTS AND MEASUREMENTS

Run No.	Model No.	Preweight, gm	Prelength, in.	Postweight, gm	Postlength, in.
S-8	ATJ-S1	6.2270	1.6093	5.5950	1.3905
	ATJ-S2	6.2182	1.0670	5.5972	1.3898
	IP-22E-67-2	5.4996	1.6060	4.8624	1.3627
	IP-22E-68-2	5.5322	1.6062	4.9276	1.3845
	IP-22C-71-2	5.4219	1.6062	4.7837	1.3658
S-9	ATJ-S3	6.1987	1.6060	5.3006	1.3880
	ATJ-S4	6.2142	1.6075	5.4274	1.4523
	IP-17-26-1	5.3522	1.6049	4.9528	1.4547
	IP-17-27-1	5.5844	1.6059	5.0546	1.4528
	IP-17-66-1	5.5417	1.6015	5.1419	1.4635
S-10A	IP-22E-67-1	5.4213	1.6057	5.0849	1.4950
	IP-22E-68-1	5.3923	1.6045	5.0696	1.4935
	IP-22F-69-1	5.8850	1.6037	5.4986	1.5031
	IP-22C-70-1	5.6679	1.6077	4.8167	1.3962
	IP-22C-71-1	5.5250	1.6078	4.6654	1.3762
S-11	ATJ-S5	6.2328	1.6085	5.3987	1.3761
	5Q-12	6.1686	1.6055	5.7346	1.4983
	5Q-22	7.2402	1.6155	6.9383	1.5385
	IP-22E-67-3	5.3939	1.6057	4.6699	1.3852
	IP-22E-68-2F	5.3660	1.6058	4.6171	1.3723
S-12A	ATJ-S6	6.2137	1.6085	5.0641	1.4393
	CVD-1-A	6.3685	1.6090	5.2545	1.2914
	IP-22E-67-4	5.4637	1.6060	5.0830	1.4521
	IP-22F-69-2	5.9168	1.6055	5.2397	1.4380
	IP-22F-69-3	5.8745	1.6036	5.2333	1.4676
S-13	ATJ-S7	6.2209	1.6092	5.4866	1.3912
	ATJ-S8	6.2338	1.6067	5.4915	1.3756
	CVD-1B	6.3512	1.6105	5.1615	1.2613
	IP-22F-69-4	5.9555	1.6060	5.2185	1.3816
	IP-22C-70-3	5.5695	1.6066	4.8112	1.3523

TABLE III
MODEL LOG

Run No.	Model No.	Model Configuration	Model Type	Sting Position	Exposure Time, sec
S-8	ATJ-S1	Hemisphere-Cylinder	Ablation	1	2.59
	ATJ-S2	Hemisphere-Cylinder	Ablation	2	2.58
	IP-22E-67-2	Hemisphere-Cylinder	Ablation	3	2.59
	IP-22E-68-2	Hemisphere-Cylinder	Ablation	4	2.57
	IP-22C-71-2	Hemisphere-Cylinder	Ablation	5	2.63
S-9	ATJ-S3	Hemisphere-Cylinder	Ablation	1	2.13
	ATJ-S4	Hemisphere-Cylinder	Ablation	2	2.05
	IP-17-26-1	Hemisphere-Cylinder	Ablation	3	2.04
	IP-17-27-1	Hemisphere-Cylinder	Ablation	4	2.14
	IP-17-66-1	Hemisphere-Cylinder	Ablation	5	2.15
S-10A	IP-22E-67-1	Hemisphere-Cylinder	Ablation	1	2.07
	IP-22E-68-1	Hemisphere-Cylinder	Ablation	2	2.08
	IP-22F-69-1	Hemisphere-Cylinder	Ablation	3	2.14
	IP-22C-70-1	Hemisphere-Cylinder	Ablation	4	2.07
	IP-22C-71-1	Hemisphere-Cylinder	Ablation	5	2.13
S-11	ATJ-S5	Hemisphere-Cylinder	Ablation	1	1.62
	5Q-12	Hemisphere-Cylinder	Ablation	2	1.65
	5Q-22	Hemisphere-Cylinder	Ablation	3	1.60
	IP-22E-67-3	Hemisphere-Cylinder	Ablation	4	1.68
	IP-22E-68-2F	Hemisphere-Cylinder	Ablation	5	1.62
S-12	ATJ-S6	Hemisphere-Cylinder	Ablation	1	1.59
	CVD-1-A	Hemisphere-Cylinder	Ablation	2	1.57
	IP-22E-67-4	Hemisphere-Cylinder	Ablation	3	1.62
	IP-22F-69-2	Hemisphere-Cylinder	Ablation	4	1.66
	IP-22F-69-3	Hemisphere-Cylinder	Ablation	5	1.63
S-13	ATJ-S7	Hemisphere-Cylinder	Ablation	1	2.06
	ATJ-S8	Hemisphere-Cylinder	Ablation	2	2.06
	CVD-1B	Hemisphere-Cylinder	Ablation	3	2.09
	IP-22F-69-4	Hemisphere-Cylinder	Ablation	4	2.08
	IP-22C-70-3	Hemisphere-Cylinder	Ablation	5	2.11

TABLE IV
ARC HEATER DATA

Run No.	Mach No.	Voltage, V, volts	Current, I, amp	$\dot{m}$, lb/sec	p_t, atm	h_t, Btu/lb	η, %	p_s,* atm
S-8	2.0	4370	735	0.406	51.1	3430	44.3	35
S-9	2.3	7500	670	0.866	99.3	2440	42.7	56
S-10A	2.3	7510	670	0.897	99.9	2455	44.2	56
S-11	1.6	6735	670	0.848	89.9	2315	44.0	76
S-12A	1.6	7375	670	0.818	90.4	2495	41.8	76
S-13	1.6	4785	725	0.461	53	3435	46.8	45

*Estimated model stagnation pressure

TABLE V
SPECIMEN RECESSION AND MASS LOSS

Run No.	Model No.	Exposure Time, Δt_m, sec	Mass Change, Δm, gm	Length Change, ΔL, in.	Loss Rate, $\Delta m/\Delta t_m$ gm/sec	Recession Rate, $\Delta L/\Delta t_m$ in./sec
S-8	ATJ-S1	2.59	0.6320	0.2188	0.2440	0.0845
	ATJ-S2	2.58	0.6210	0.2172	0.2407	0.0842
	IP-22E-67-2	2.59	0.6372	0.2433	0.2460	0.0939
	IP-22E-68-2	2.57	0.6046	0.2217	0.2352	0.0863
	IP-22C-71-2	2.63	0.6382	0.2404	0.2426	0.0914
S-9	ATJ-S3	2.13	0.8981	0.2180	0.4216	0.1023
	ATJ-S4	2.05	0.7868	0.1552	0.3838	0.0757
	IP-17-26-1	2.04	0.3994	0.1502	0.1958	0.0736
	IP-17-27-1	2.14	0.5298	0.1531	0.2476	0.0715
	IP-17-66-1	2.15	0.3998	0.1380	0.1859	0.0642
S-10A	IP-22E-67-1	2.07	0.3364	0.1107	0.1625	0.0535
	IP-22E-68-1	2.08	0.3227	0.1110	0.1551	0.0534
	IP-22F-69-1	2.14	0.3864	0.1006	0.1805	0.0470
	IP-22C-70-1	2.07	0.8512	0.2115	0.4112	0.1022
	IP-22C-71-1	2.13	0.8596	0.2316	0.4035	0.1087
S-11	ATJ-S5	1.62	0.8341	0.2324	0.5149	0.1434
	5Q-12	1.65	0.4340	0.1072	0.2630	0.0650
	5Q-22	1.60	0.3019	0.0770	0.1887	0.0481
	IP-22E-67-3	1.68	0.7240	0.2205	0.4309	0.1312
	IP-22E-68-2F	1.62	0.7489	0.2335	0.4622	0.1441
S-12A	ATJ-S6	1.59	1.1496	0.1692	0.7230	0.1064
	CVD-1-A	1.57	1.1140	0.3176	0.7095	0.2023
	IP-22E-67-4	1.62	0.3807	0.1539	0.2350	0.0950
	IP-22F-69-2	1.66	0.6771	0.1675	0.4079	0.1009
	IP-22F-69-3	1.63	0.6412	0.1360	0.3934	0.0834
S-13	ATJ-S7	2.06	0.7343	0.2180	0.3564	0.1058
	ATJ-S8	2.06	0.7423	0.2311	0.3603	0.1122
	CVD-1B	2.09	1.1897	0.3492	0.5692	0.1671
	IP-22F-69-4	2.08	0.7370	0.2244	0.3543	0.1079
	IP-22C-70-3	2.11	0.7583	0.2543	0.3594	0.1205

TABLE VI
PYROMETER DATA

Run No.	Model No.	Temperature Pyrometer No. 27 °R
S-8	ATJ-S1	5625
	ATJ-S2	5600
	IP-22E-67-2	5600
	IP-22E-68-2	5600
	IP-22C-71-2	5600
S-9	ATJ-S3	5150
	ATJ-S4	5200
	IP-17-26-1	5050
	IP-17-27-1	4975
	IP-17-66-1	4975
S-10A	IP-22E-67-1	5285
	IP-22E-68-1	5325
	IP-22F-69-1	5175
	IP-22C-70-1	5500
	IP-22C-71-1	5425
S-11	ATJ-S5	5650
	5Q-12	5625
	5Q-22	5575
	IP-22E-67-3	5525
	IP-22E-68-2F	5635
S-12A	ATJ-S6	5625
	CVD-1-A	5710
	IP-22E-67-4	5550
	IP-22F-69-2	5575
	IP-22F-69-3	5650
S-13	ATJ-S7	5425
	ATJ-S8	5450
	CVD-1B	5485
	IP-22F-69-4	5425
	IP-22C-70-3	5325

UNCLASSIFIED

Security Classification

DOCUMENT CONTROL DATA - R & D

(Security classification of title, body of abstract and indexing annotation must be entered when the overall report is classified)

1. ORIGINATING ACTIVITY *(Corporate author)*
Arnold Engineering Development Center
ARO, Inc., Operating Contractor
Arnold Air Force Station, Tennessee

2a. REPORT SECURITY CLASSIFICATION
UNCLASSIFIED

2b. GROUP
N/A

3. REPORT TITLE
SANDIA HIGH-PRESSURE ABLATION TEST IN THE AEDC 5-MEGAWATT ARC HEATER TEST UNIT SERIES III

4. DESCRIPTIVE NOTES *(Type of report and inclusive dates)*
June 3 to June 7, 1968 - Final Report

5. AUTHOR(S) *(First name, middle initial, last name)*
J. R. Henson, ARO, Inc.

6. REPORT DATE	7a. TOTAL NO OF PAGES	7b. NO OF REFS
September 1968	42	2

8a. CONTRACT OR GRANT NO
F40600-69-C-0001

b. PROJECT NO

c. Program Area 920D

d.

9a. ORIGINATOR'S REPORT NUMBER(S)
AEDC-TR-68-192

9b. OTHER REPORT NO(S) *(Any other numbers that may be assigned this report)*
N/A

10. DISTRIBUTION STATEMENT This document is subject to special export controls and each transmittal to foreign governments or foreign nationals may be made only with prior approval of AEC, Albuquerque Oprs Office, P. O. Box 5400, Albuquerque, New Mexico 87115.

11. SUPPLEMENTARY NOTES
Available in DDC

12. SPONSORING MILITARY ACTIVITY
AEC, Albuquerque Oprs Office,
P. O. Box 5400,
Albuquerque, New Mexico 87115

13. ABSTRACT

Six ablation test runs, involving 30 models, were made in an arc-heated free-jet facility using air as the test fluid. The test was conducted to screen and examine the ablation performance of various materials with different microscopic structures. The investigation was accomplished at Mach numbers of 1.6, 2.0, and 2.3 with measured reservoir pressures ranging from 51.1 to 99.0 atm and enthalpies from 3435 to 2315 Btu/lb. The models were hemisphere-cylinder specimens of composite materials. The data measured during the present investigation are presented in a documentary manner with a minimum of analysis because the composition of the specimen material is proprietary. The models are referred to by number designation only.

This document is subject to special export controls and each transmittal to foreign governments or foreign nationals may be made only with prior approval of AEC, Albuquerque Oprs Office, P. O. Box 5400, Albuquerque, New Mexico 87115.

This document has been approved for public release its distribution is unlimited. Per AF Letter dtd 23 Jan., 75 signed William O. Cole.

DD FORM 1 NOV 65 1473

UNCLASSIFIED

Security Classification

14 KEY WORDS	LINK A		LINK B		LINK C	
	ROLE	WT	ROLE	WT	ROLE	WT
materials						
ablation						
pressure effects						
temperature effects						
supersonic flow						
arc-heater test facilities -- PWT						
blunt bodies						
conical bodies						

~~1~~
2 5-Megawatt arc heater. Test facility -- PWT.
3 Hemisphere cylinders
4 Blunt nosed bodies -- Ablation.
5. Ablation -- ablation
6. Composites
15-7.